

Contemporary crustal velocity field in Alpine Mediterranean area of Italy from new geodetic data

Gregorio Farolfi^{1,2}  · Chiara Del Ventisette¹

Received: 26 May 2015 / Accepted: 31 July 2015

© The Author(s) 2015. This article is published with open access at Springerlink.com

Abstract A new crustal velocity field for the Alpine Mediterranean area was determined by using a time series spanning 6.5 years of 113 global navigation satellite system (GNSS) permanent stations. This area is characterized by a complex tectonic setting driven by the interaction of Eurasian and African plates. The processing was performed by using a state-of-the-art absolute antenna phase center correction model and by using recomputed precise International GNSS Service orbits, available since April 2014. Thus, a new and more accurate tropospheric mapping function for geodetic applications was adopted. Results provide a new detailed map of the kinematics throughout the entire study area. In some area of the Italian peninsula, such as in the central Apennines, the velocity vector orientation appears rotated with respect to previous results. These discrepancies suggest that the geodynamic setting of this sector of Mediterranean area should be revised in accordance with these new results.

Keywords GNSS permanent stations · IGS08 calibrations · Crustal velocity field · Euler pole · Alpine Mediterranean region

Introduction

GNSS permanent stations networks are the most common geodetic technique used to materialize and distribute the global geodetic reference system (i.e., International Terrestrial Reference System—ITRS). GNSS continuous time series analyses have made significant contributions in monitoring temporal and spatial changes in the earth's lithosphere and atmosphere.

The aim of this work is to calculate and analyze the spatial variations of continuous time series of GNSS permanent stations and, finally, to estimate crustal velocities in the Alpine Mediterranean area, which can be used to test and substantiate actual geodynamical hypotheses.

Much scientific literature is available for the velocity field of this area from space geodesy (Noquet 2012). Most of these studies are based on static GPS techniques performed in separated single campaigns during a period of many years. Today, the large number of GNSS permanent stations already existing in the study area allows continuous monitoring of the permanent stations with higher accuracy and higher temporal resolution compared with static GNSS campaigns.

The dataset is composed of 113 GNSS permanent stations, including eight International GNSS Service (IGS) stations that provide datum alignment. The observation window spans 6.5 years, from January 2008 to June 2014.

The adopted processing strategy follows the 2010 International Earth Rotation and Reference Systems Service (IERS) conventions. A state-of-the-art tropospheric empirical global mapping function (Böhm et al. 2007) was applied to map the tropospheric delay in the zenith direction.

Two important contributions to this work are new antenna phase center calibrations and recomputed IGS

✉ Gregorio Farolfi
gregorio.farolfi@gmail.com
Chiara Del Ventisette
chiara.delventisette@unifi.it

¹ Department of Earth Sciences, University of Firenze, Via La Pira 4, 50121 Florence, Italy

² Istituto Geografico Militare, Via Battisti, 10/12, 50121 Florence, Italy

orbits. The new absolute phase center model for both the receiver and the satellite antennas, called `igs08.atx`, is more precise and accurate than the older `igs05.atx` model. The new antenna calibration was introduced by IGS since GPS week 1632 (April 17, 2011) and it produced a discontinuity in the positional time series. For this reason, the Center for Orbit Determination in Europe (CODE) recomputed precise IGS orbits (`.sp3`) from 1994 to 2013 and made them available since April 2014. Thus, results obtained are fully consistent with the IGB08 international reference frame. Coordinate time series were analyzed to identify and remove discontinuities. Velocities were computed by applying the linear regression method. In order to highlight intra-plate motions of the area of study, the velocity field was transformed into the Eurasian reference frame (i.e., European Terrestrial Reference System—ETRS89). The resulting velocity field shows the structural and kinematic complexity in the Alpine Mediterranean area and improves the framework for analyzing the dynamic processes governing crustal deformation.

Network and data description

The primary geodetic contribution to the project is the high number of GNSS permanent stations already existing in Alpine Mediterranean area and their data availability (Fig. 1). Selected stations present redundancy and temporal continuity, good documentation and homogeneous distribution belonging to national and European geodetic networks. Data analysis was performed using 113 GNSS permanent stations, including all the active stations of the Italian geodetic network (Baroni et al. 2009), 35 stations belonging to the European Permanent Network (EPN) and 8 stations to the IGS network for datum alignment. Moreover, 11 of these EPN stations are defined by EUREF as ‘Class A,’ and they present a long time series solutions in IGB08 calculated from GPS week 834–1800 (January 1996–July 2014). The observation windows are composed by a single weekly solution every month from GPS week 1460–1799 and covering a period of 6.5 years, from January 1, 2008 to June 30, 2014.

GNSS data processing

Quality check of the data was carried out using TEQC software developed by UNAVCO (Estey and Meertens 1999), and the processing was performed with Bernese GPS Software (Dach et al. 2007) from the Astronomical Institute of the University of Bern (AIUB). The processing strategy followed the most recent EUREF guidelines (2013) for local analysis centers. Data were semi-automatically processed

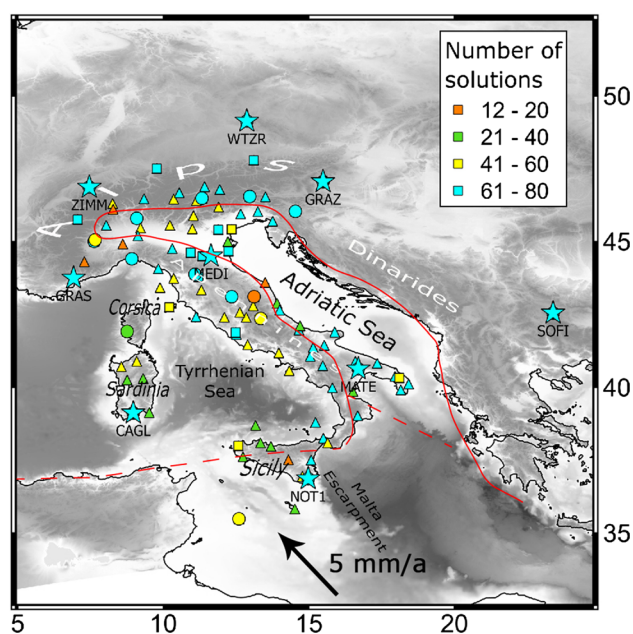


Fig. 1 Map of GNSS permanent stations and their data availability. Stars represent the global IGS reference stations used for the datum alignment. Squares show EPN stations, built to materialize and maintain the European Terrestrial Reference System (ETRS89). Circles are ‘Class A’ EPN stations, identified by a high quality and long continuity of data. Triangles show geodetic stations belonging to local institutions, built to provide real-time kinematic signals or cadastral purposes. Symbols are colored based on the number of weekly solutions obtained for each station. The red lines separate the African plate, Adria plate and Eurasian plate (Weber et al. 2010); the black arrow indicates the velocity vector ($v_\phi = 3.5$ mm/a, $v_\lambda = -3.5$ mm/a) of the Nubia plate in Eurasia-fixed reference frame. Convergence of Nubia plate to Eurasia has been determined applying the following Euler pole parameters calculated from Altamimi et al. (2012); $\phi_{\text{Eurasia}} = 54.2^\circ$, $\lambda_{\text{Eurasia}} = -98.8^\circ$, $\Omega_{\text{Eurasia}} = 0.257^\circ/\text{Ma}$, $\phi_{\text{Nubia}} = 49.8^\circ$, $\lambda_{\text{Nubia}} = -81.0^\circ$, $\Omega_{\text{Nubia}} = 0.262^\circ/\text{Ma}$

using the Bernese Processing Engine (BPE) except for the normal equation stacking stage.

Each daily session was processed independently. The main features of the processing strategy are the interstation baselines formulated using an automated procedure based on a maximum-number-of-observation strategy with a maximum baseline length of 200 km. Data were cleaned by removing observations with elevation angles $< 3^\circ$, unpaired observations, and short data periods. Resolution of ambiguities was performed with QIF (Quasi-Ionosphere-Free) algorithm. The QIF strategy is used to solve ambiguities of baselines over several hundred kilometers. The criterion is to minimize the difference between the real-valued and integer ionospheric-free biases applied to single differences (Dach et al. 2007).

Tropospheric delay in zenith direction was calculated with a priori zenith hydrostatic delay (ZHD) model. The zenith wet delay (ZWD) was estimated using the global model of pressure and temperature for geodetic

applications (GMT) developed by Böhm et al. (2007). Daily solutions were obtained using double difference level, multi-base processing with tropospheric delays estimated every 1 h with wet GMT function. Stations with a RMS higher than 20 mm for the north and east components and higher than 40 mm for the up component were eliminated, and the daily datasets were re-computed. Daily free normal equation solutions are stacked to produce a single weekly normal equation. For alignment to the datum, reference stations coordinates are a priori estimated for the dataset epoch using a set of coordinates and velocities defined in the IGb08 global reference frame. Then, each weekly normal equation is aligned to the IGb08 frame by minimizing the differences between calculated and a priori estimated coordinates of reference stations using a Helmert transformation with only three translation parameters.

The IGb08 reference frame represents a specific GNSS realization of the ITRF2008. It was adopted by IGS on April 17, 2011 (GPS week 1632), together with the igs08.atx antenna phase center model (IGSMAIL 6354 and 6355, Upcoming switch to IGS08/igs08.atx). Even if the coordinates of some stations are different in IGb08 and ITRF2008, the global Helmert transformation from ITRF2008 to IGb08 should be considered zero. Both frames are indeed based on the same underlying datum (Rebischung et al. 2012).

Time series analysis

Weekly positioning solutions produce time series for each of the three sites coordinates. As a first approximation, linear regression trends derived from coordinate time series generate velocities. In order to obtain more accurate results, annual and semi-annual seasonal effects were calculated, discontinuities in the time series were detected and analyzed, and obvious outliers were removed. An automated recursive procedure was applied to each station to detect discontinuities and calculate offset corrections. Probable discontinuities were identified and highlighted comparing their values to predicted thresholds. In most cases, the detected discontinuities were due to antenna changes. The least-squares approach was applied independently to each site modeling the position components $Y_k(t_i)$ at epoch t_i by the following relation:

$$Y_k(t_i) = Y_k(t_0) + v_k \cdot (t_i - t_0) + \sum_{p=1}^2 a_p \cdot \cos(2p\pi t_i + \varphi_p) + \sum_{j=1}^J d_j \cdot \Theta(t_j - t_i) \tag{1}$$

where $k = n, e, u$ for north, east and up components, $Y_k(t_0)$ is the station position at time t_0 , v_k is the velocity of k component from best fitting line after removing periodic

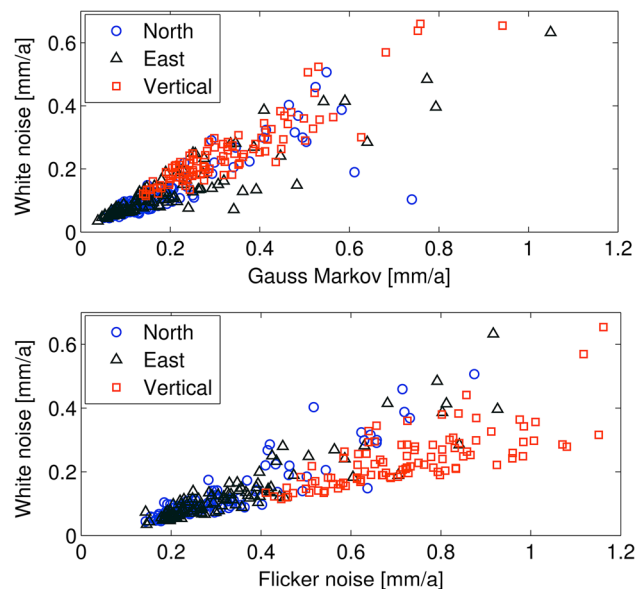


Fig. 2 Estimated velocity uncertainties using spectral analysis (CATS) and Gauss–Markov fitting of averages. *Top*—White noise versus first order of Gauss–Markov uncertainties. *Bottom*—White noise versus flicker noise. *Blue circles, black triangles and red squares* represent, respectively, the errors of the north, east and vertical components

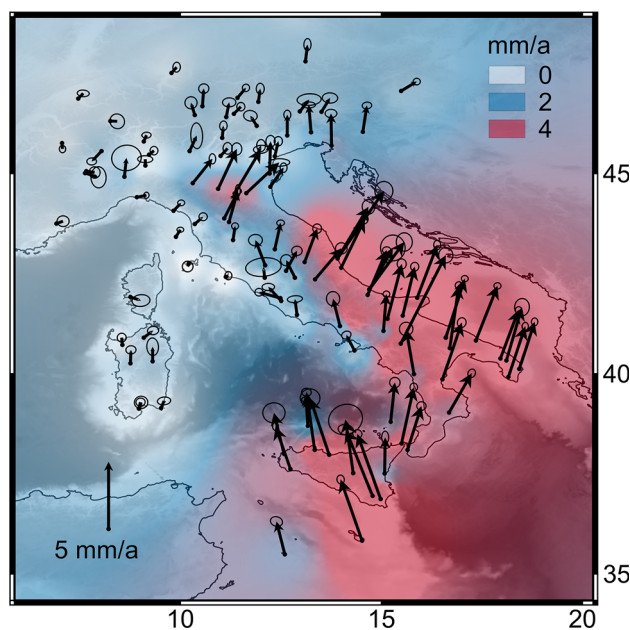


Fig. 3 Intra-plate horizontal velocities and error ellipses of 95 % confidence level in the Eurasian reference frame. Interpolated horizontal velocity field is displayed by a graduated color scale. *White* represents stable part, *blue* 2 mm/a and *red* up to 4 mm/a

signal and discontinuities, a_1 and φ_1 are annual amplitude and phase, a_2 and φ_2 are semi-annual amplitude and phase, d_j is discontinuity introduced at epoch t_j and $\Theta(t) = 0$ if $t < 0$ and $\Theta(t) = 1$ if $t \geq 0$.

Formal velocity error statistics estimated with a standard least square algorithm underestimate actual values (Zhang

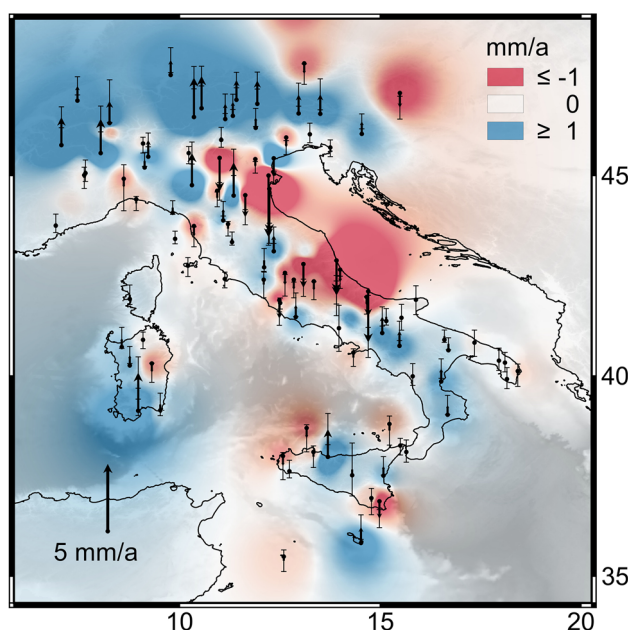


Fig. 4 Vertical velocities and error bars with 95 % confidence level. The interpolated vertical velocity field is displayed by a graduated color scale. *White* represents stable area, *blue* is for uplift ≥ 1.0 mm/a and *red* subsidence ≤ -1.0 mm/a

et al. 1997; Mao et al. 1999). The assumptions of stationary are often not valid, and rate standard deviations are dependent on the low frequency part of the noise spectrum which is poorly determined. More realistic uncertainties of the estimated velocities must account for the correlated noise present in the time series. Annual and semi-annual periodic signals were previously examined to avoid a biased adjustment. The analysis of correlated noise was performed using the maximum likelihood estimation (MLE) technique (CATS software, Williams 2008). Power law noise models and first order of Gauss–Markov process were analyzed and compared with each other (Fig. 2). The rate uncertainties appear clearly correlated in all the three direction components. A straight line fits to the points with a scale factor of 1–2 between white noise and Gauss–Markov uncertainty, while a scale factor of 2–4 between white and flicker noise. Finally, realistic velocity uncertainties were estimated using a combination of white noise plus flicker noise (Williams 2003; Williams et al. 2004).

Velocities estimation in the European Terrestrial Reference System (ETRS)

The ITRF08/IGS08 velocity field map is not well suited to give an easy overview and interpretation of the geodynamic of the study area. The intra-plate horizontal site velocity V_E was computed for each site by subtracting the point velocity $V_I = (v_{xI}, v_{yI}, v_{zI})$ whose position vector is

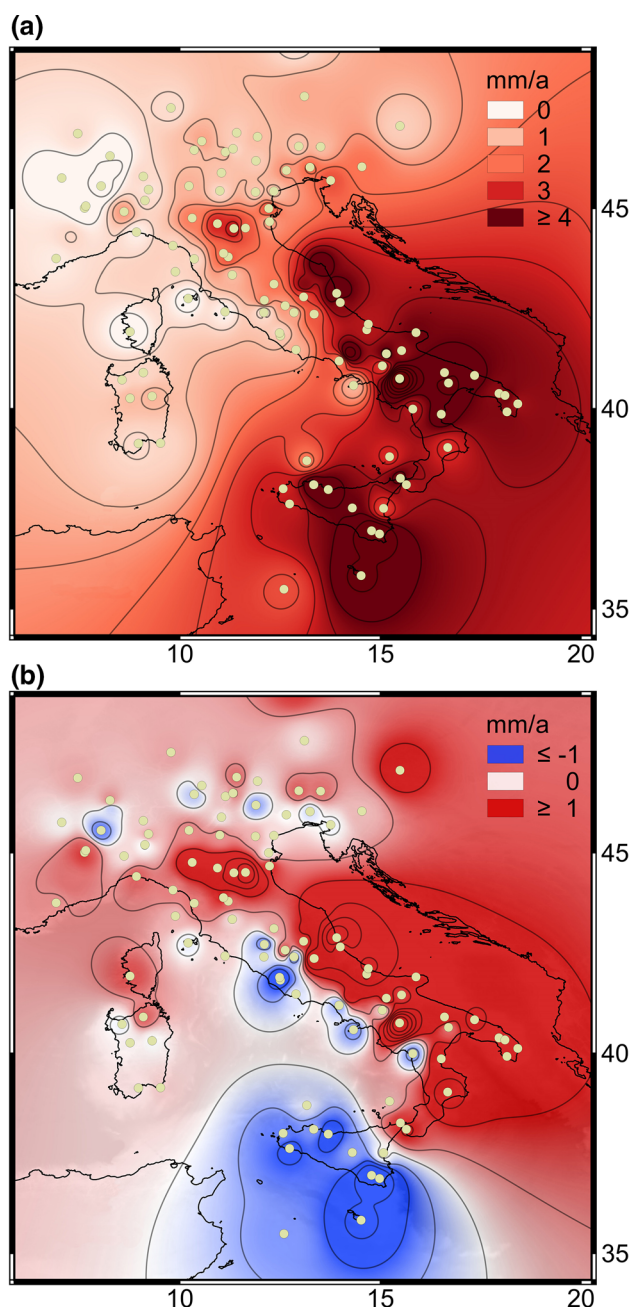


Fig. 5 Velocity field components contour plot. *Top*—North component; in *red* scale color are plotted displacements toward north; no movements toward south are recorded. *Bottom*—East component; values in *red* indicate movement toward east, while values in *blue* toward west; the relative stability is plotted in *white*

$P = (X, Y, Z)$, and the absolute rigid plate kinematic model for the Eurasia plate $V_{Eurasia\ plate}$

$$V_E = V_I - V_{Eurasia\ plate} = V_I - \Omega \times P$$

$$= \begin{bmatrix} v_{xI} \\ v_{yI} \\ v_{zI} \end{bmatrix} - \begin{bmatrix} 0 & Z & -Y \\ -Z & 0 & X \\ Y & -X & 0 \end{bmatrix} \begin{bmatrix} \omega_x \\ \omega_y \\ \omega_z \end{bmatrix} \quad (2)$$

Table 1 Difference of velocities in mm/a between computed and ‘Class A’ EPN solutions. These stations identify a high quality with long continuity of data (more than 18 years of continuous observations)

Station	Lat	Lon	North (mm/a)	East (mm/a)	Up (mm/a)
AJAC	41.9274	8.7626	0.4	0.4	-0.5
AQUI	42.3682	13.3502	-0.8	1.0	-0.9
BZRG	46.4990	11.3367	-0.3	0.6	-0.3
CAGL	39.1359	8.9727	0.2	-0.1	0.1
CAGZ	39.1358	8.9727	2.0	0.3	2.0
CAME	43.1119	13.1239	-0.5	-0.7	-0.2
COMO	45.8021	9.0956	-0.3	0.1	-0.1
GENO	44.4193	8.9211	-0.1	0.1	-0.2
GRAZ	47.0671	15.4934	-0.9	-0.1	-1.0
GSR1	46.0481	14.5437	0.7	0.2	0.3
IENG	45.0151	7.6394	-0.1	0.2	-0.4
LAMP	35.4997	12.6056	-0.5	2.0	-1.0
MATE	40.6491	16.7044	-0.3	-0.5	-0.1
NOT1	36.8758	14.9897	-0.4	-0.4	-0.5
PRAT	43.8855	11.0991	0.4	0.2	0.3
SOFI	42.556	23.3947	0.2	-0.7	0.4
TORI	45.0633	7.6612	-0.3	0.2	-0.8
UNPG	43.1193	12.3557	0.2	-0.2	0.1
WTZR	49.1441	12.8789	-1.0	0.1	-0.9
ZIMM	46.877	7.4652	0.2	-0.01	-0.2
ZOUF	46.5572	12.9735	-0.02	0.1	-0.3
Mean			-0.03	0.1	-0.2
Absolute mean			0.5	0.4	0.5
Root mean square			0.5	0.4	0.6

From left to the right: four characters site code, longitude, latitude and differences in north and east components

Table 2 ITRF2008 absolute frame rotation vectors and poles

Frame	ω_x (mas/a)	ω_y (mas/a)	ω_z (mas/a)	Ω (°/Ma)	Lat (°)	Lon (°)
ALP-MED	0.1034 ± 0.008	-0.541 ± 0.008	0.945 ± 0.008	0.30393 ± 0.002	59.8	-79.1
EURA	-0.083 ± 0.008	-0.534 ± 0.007	0.750 ± 0.008	0.257 ± 0.002	54.2	-98.8

The three Cartesian components of the Eurasia Euler pole relative to IGB08 are $\omega_x = -0.083$, $\omega_y = -0.534$ and $\omega_z = 0.775$ mas/a, published by Altamimi et al. (2012).

The estimated horizontal velocities with 95 % confidence error ellipses are shown in Fig. 3, and the vertical velocities with error bars are shown in Fig. 4. In order to gain further insights into the kinematic processes, we computed interpolated horizontal and vertical velocity fields within a regular grid ($0.02^\circ \times 0.02^\circ$). The interpolation was computed by applying inverse distance weighting (Shepard 1968), a deterministic multivariate method with a set of scattered points. The weight of any known point is set inversely proportional to its distance from the interpolated (unknown) point as $w(d) = d^{-2}$.

Maps of variation for the north and east components of velocity field are shown in Fig. 5.

In order to verify the above velocities, they were compared with the velocities of 11 ‘Class A’ EPN stations. These velocities are the cumulative combination of 18.5 years of weekly solutions, from GPS week 834 until 1800. Processing of ‘Class A’ EPN stations was performed by Kenyeres (2014) applying recomputed precise IGS08 orbits and igs08.atx antenna phase center model. Absolute mean differences between datasets are 0.5 mm/a and 0.4 mm/a, respectively, for the north and east components (Table 1). This comparison shows that computed velocities are very close to the velocities determined from a wider dataset spanning 18.5 years.

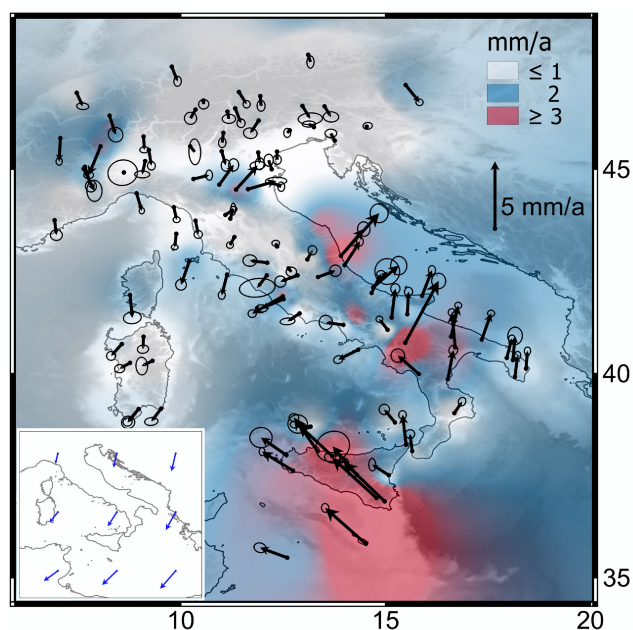


Fig. 6 Horizontal velocities and error ellipses (95 % of confidence level) in the local reference frame defined for the Alpine Mediterranean area. The interpolated horizontal velocity field is displayed by a graduated color scale. *White* represents stable part, *blue* 2 mm/a and *red* up to 4 mm/a. Velocity field vectors of the Alpine Mediterranean Euler Pole with respect to the Eurasia are shown in the *inset*

Euler rotation vector and Euler pole for the Alpine Mediterranean area

The Alpine Mediterranean area shows a relative velocity residual to the stable part of Eurasia plate. GNSS stations located in Sicily largely present a velocity up to 4 mm/a, in agreement with the Eurasia–Nubian convergence process (Hollenstein et al. 2003). Since the ETRS velocity field map does not show an easy overview and interpretation of the geodynamic pattern of the study area, a local reference frame was defined. A local frame is identified with a relative movement or rotation with respect to another one. It is described by a relative kinematic model or applying a rotation for angle Ω around a point on earth's surface, i.e., the Euler pole. The intersection of the Euler pole on the surface of the earth is a fixed point around which the frame rotates. The Euler rotation model essentially constrains the frame to move rigidly on the earth surface, without changing vertical velocities. The determination of the local frame for the case of study was performed using all the site velocities of the network and their errors in the ITRF2008/IGb08 reference frame, by estimating the three Euler vector parameters (Table 2) that minimize the horizontal components of velocity with a weighted least-squares inversion (Perez et al. 2003). The computed velocity field is displayed in Fig. 6, and its horizontal components are shown in Fig. 7.

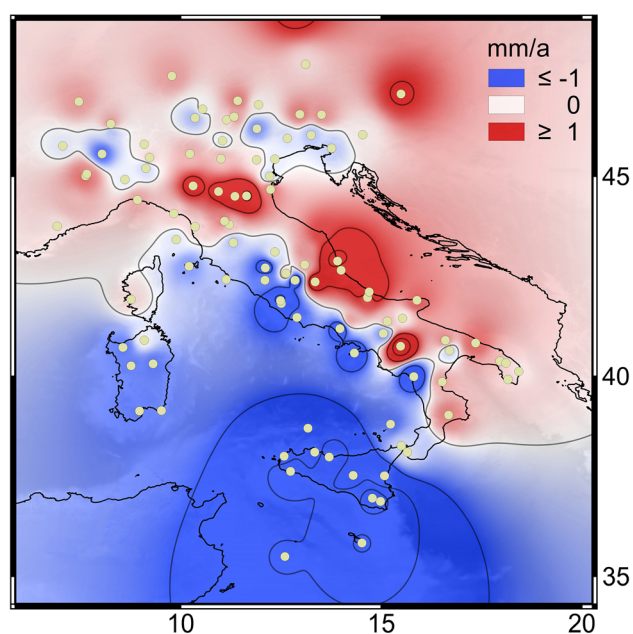
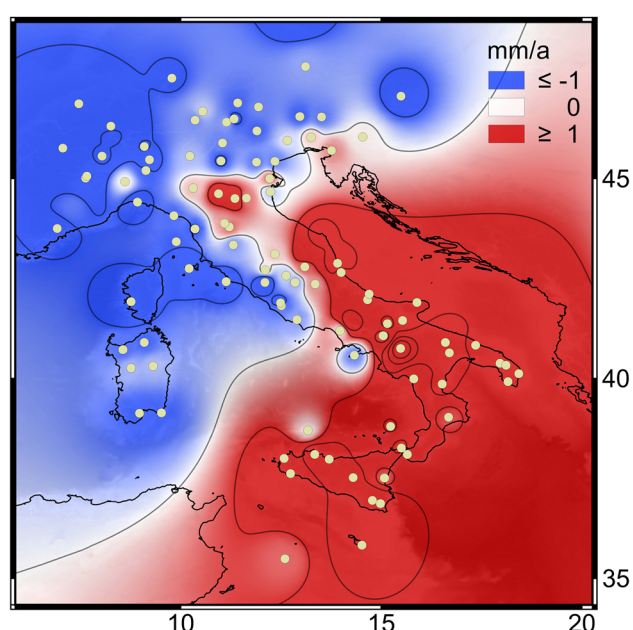


Fig. 7 Velocity field components contour plot in the local reference frame defined for Alpine Mediterranean area. *Top*—North component; in *red* scale color are plotted displacements toward north; in *blue* toward south. *Bottom*—East component; values in *red* indicate movement toward east, while values in *blue* toward west; the relative stability is plotted in *white*

Discussion and Conclusions

The new processing of the permanent GNSS data, performed by using a state-of-the-art absolute antenna phase center correction model and by using recomputed precise IGS orbits allows evaluating the crustal velocity field of the Italian Peninsula with horizontal component errors

generally <0.2 mm/a. The results show that the velocity field along the west Alpine chain does not show significant residual motion relative to the Eurasian plate (<0.2 mm/a). The main deformation of this area is connected with uplift that reaches a mean value of 1 mm/a, generally lower than the computational error (Fig. 4). Small residual motions arise along the northern Apennines and on the nearby Po plain. The Apennine axis constitutes a boundary zone between two different velocity patterns; the inner Apennine is almost stable relative to Eurasia, while the outer sector shows a velocity field of 3–5 mm/a in NE direction. In the central Apennines, the velocity vector orientation appears rotated more than 30° clockwise with respect to previous data (Serpelloni et al. 2005; Angelica et al. 2013; Cenni et al. 2012). Southern Italy shows the greatest residual motions compared to the Eurasian plate. An important boundary line that separates peninsular Italy from Sicily presents different velocity patterns (Figs. 3 and 5) that assume a fan-shaped divergent motions (Hollenstein et al. 2003) showing a minor fan-shaped angle with respect to previous data; for example, in western Sicily our data show a 13° clockwise rotation of the velocity vector with respect the vector given by Palano (2015); in eastern Sicily, it shows a 15° counterclockwise rotation. The western part of Sicily shows 5.0 mm/a velocities in direction NNW, while eastern Sicily and Calabria move at slower rate of 3.5 mm/a in NE direction (Fig. 5a). Western Sicily shows a faster north component of 1.5 mm/a and presents a relative E–W stretching of 2.5 mm/a with respect to Calabria (Fig. 5b) where our data mostly replicate the velocity field previously detected (Ventura et al. 2014). The eastern Alps, Corsica, Sardinia and the Tyrrhenian Sea (which is covered only by interpolation data) show small velocity residuals with respect to the Eurasian plate.

The velocity field estimated using the local reference frame (Alpine Mediterranean area) highlights the movements toward the north of the central and southern Apennine, while the Alpine chain and the Sardinia–Corsica block moved relatively to the south. The east–west velocity component confirms that the inner Apennines moved toward west, conversely the outer Apennines which move relatively to the east. These patterns, also taking into account the component velocity modulus, identify the main boundary zones in the Italian peninsula.

The new GNSS data document a complex pattern of crustal motion characterized by divergent orientation of velocity vectors, especially in central/southern Apennines, Calabrian arc and Sicily that highlight a strong tectonic fragmentation of these areas. The actual geodynamic setting of this sector of Mediterranean area

should be revised taking into account these new GNSS data.

Acknowledgments This work was supported by Istituto Geografico Militare (IGM) and Department of Earth Sciences, University of Firenze (Professor N. Casagli). Fruitful discussions and exchanges with W. Frodella and A. Piombino have been very valuable for the work. All the figures were prepared using the open source Quantum GIS.

Open Access This article is distributed under the terms of the Creative Commons Attribution 4.0 International License (<http://creativecommons.org/licenses/by/4.0/>), which permits unrestricted use, distribution, and reproduction in any medium, provided you give appropriate credit to the original author(s) and the source, provide a link to the Creative Commons license, and indicate if changes were made.

References

- Altamimi Z, Métivier L, Collilieux X (2012) ITRF2008 plate motion model. *J Geophys Res* 117(B07402). doi:10.1029/2011JB008930
- Angelica C, Bonforte A, Distefano G, Serpelloni E, Gresta S (2013) Seismic potential in Italy from integration and comparison of seismic and geodetic strain rates. *Tectonophysics* 608:996–1006. doi:10.1016/j.tecto.2013.07.014
- Baroni L, Cauli F, Farolfi G, Maseroli R (2009) Final results of the Italian Rete Dinamica Nazionale (RDN) of Istituto Geografico Militare Italiano (IGMI) and its alignment to ETRF2000. *Bull Geod Geomat* 68(3):287–320 (ISSN 0006-6710)
- Böhm J, Heinkelmann R, Schuh H (2007) A global model of pressure and temperature for geodetic applications. *J Geod* 81(10):679–683. doi:10.1007/s00190-007-0135-3
- Cenni N, Mantovani E, Baldi P, Viti M (2012) Present kinematics of Central and Northern Italy from continuous GPS measurements. *J Geodyn* 58:62–72. doi:10.1016/j.jog.2012.02.004
- Dach R, Hugentobler U, Fridez P, Meindl M (2007) The Bernese GPS Software Version 5.0. Astronomical Institute of University of Bern (AIUB), Bern
- Estey L, Meertens C (1999) TEQC: the multi-purpose toolkit for GPS/GLONASS data. *GPS solut* 3(1):42–49
- Hollenstein C, Khale HG, Geiger A, Jenny S, Goes S, Giardini D (2003) New GPS constraints on the Africa–Eurasia plate boundary zone in Southern Italy. *Geophys Res Lett* 30(18). doi:10.1029/2003GL017554
- Kenyeres A (2014) EUREF densification of the IGS08, ftp://epncb.oma.be/epncb/station/coord/EPN/EPN_A_IGb08
- Mao A, Harrison CGA, Dixon TH (1999) Noise in GPS coordinate time series. *J Geophys Res* 104(B2):2797–2816. doi:10.1029/1998JB900033
- Noquet J (2012) Present-day kinematics of the Mediterranean: a comprehensive overview of GPS results. *Tectonophysics* 579:220–242. doi:10.1016/j.tecto.2012.03.037
- Palano M (2015) On the present-day crustal stress, strain-rate fields and mantle anisotropy pattern of Italy. *Geophys J Int* 200:969–985
- Perez J, Monico J, Chaves J (2003) Velocity field estimation using GPS precise point positioning: the South American plate case. *J Glob Position Syst* 2(2):90–99
- Reischung P, Griffiths J, Ray J, Schmid R, Collilieux X, Garayt B (2012) IGS08: the IGS realization of ITRF2008. *GPS Solut* 16(4):483–494. doi:10.1007/s10291-011-0248-2

- Serpelloni E, Anzidei M, Baldi P, Casula G, Galvani A (2005) Crustal velocity and strain-rate fields in Italy and surrounding regions: new results from the analysis of permanent and non-permanent GPS networks. *Geophys J Int* 161:861–880
- Shepard D (1968) A two-dimensional interpolation function for irregularly-spaced data. *Proceedings of the 1968 ACM national conference*. pp 517–524. doi:[10.1145/800186.810616](https://doi.org/10.1145/800186.810616)
- Ventura BM, Serpelloni E, Argnani A, Bonforte A, Bürgmann R, Anzidei M, Baldi P, Puglisi G (2014) Fast geodetic strain-rates in eastern Sicily (Southern Italy): new insights into block tectonics and seismic potential in the area of the great 1693 earthquake. *Earth Planet Sci Lett* 404:77–88. doi:[10.1016/j.epsl.2014.07.025](https://doi.org/10.1016/j.epsl.2014.07.025)
- Weber J, Vrabec M, Pavlovčič-Prešeren P, Dixon T, Jiang Y, Stopar B (2010) GPS-derived motion of the Adriatic microplate from Istria Peninsula and Po Plain sites, and geodynamic implications. *Tectonophysics* 483:214–222. doi:[10.1016/j.tecto.2009.09.001](https://doi.org/10.1016/j.tecto.2009.09.001)
- Williams SDP (2003) The effect of colored noise on the uncertainties of rates estimated from geodetic time series. *J Geod* 76:483–494. doi:[10.1007/s00190-002-0283-4](https://doi.org/10.1007/s00190-002-0283-4)
- Williams SDP (2008) CATS: GPS coordinate time series analysis software. *GPS Solut* 12(2):147–153. doi:[10.1007/s10291-007-0086-4](https://doi.org/10.1007/s10291-007-0086-4)
- Williams SDP Y, Bock Y, Fang P, Jamason P, Nikolaidis RM, Prawirodirdjo L, Miller M, Johnson DJ (2004) Error analysis of continuous GPS position time series. *J Geophys Res* 109(B03412). doi:[10.1029/2003JB002741](https://doi.org/10.1029/2003JB002741)
- Zhang J, Bock Y, Johnson H, Fang P, Genrich J, Williams S, Wdowinski S, Behr J (1997) Southern California permanent GPS geodetic array: error analysis of daily position estimates and site velocities. *J Geophys Res* 102(B8):18035–18055. doi:[10.1029/97JB01380](https://doi.org/10.1029/97JB01380)



Gregorio Farolfi is a physicist at the Geodetic Bureau of the Italian Geographic Institute. He processed the Italian GNSS Geodetic Reference Network and presented it at European congresses EUREF 2009 and 2010. For many years, he has been involved in oceanographic surveys worldwide. He has also many artistic activities which lead him to receive international prizes (www.farolfiphoto.com).



Chiara Del Ventisette is a researcher at the Earth Sciences Department dell'Università di Firenze. She received a degree in Geology in 2001 and a Ph.D. in Earth Science (Structural Geology) in 2005 at the University of Florence. Her research interests include structural geology and ground deformation monitoring by means of ground-based and satellite radar interferometry.